APPLIED ORGANOMETALLIC CHEMISTRY, VOL. 12, 381–386 (1998)

Dynamical Magnetic Behavior of Interacting γ-Fe_2O_3 Particles

D. Fiorani[1], J. L. Dormann[2], F. Lucari[3]*, F. D'Orazio[3], E. Tronc[4] & J. P. Jolivet[4]
[1]IC–MAT, CNR, CP 10, 00016 Monterotondo Stazione, Italy
[2]Laboratoire de Magnétisme et d'Optique, CNRS—Université de Versailles, 45 Av. des Etats-Unis, 78035 Versailles-Cedex, France
[3]INFM and Dipartimento di Fisica, Università, 67100 L'Aquila, Italy
[4]Laboratoire de Chimie de la Matière Condensée, Université P. et M. Curie, 75252 Paris-Cedex 05, France

The dynamical behavior of γ-Fe_2O_3 particles dispersed in a polymer have been investigated by a.c. susceptibility and Mössbauer spectroscopy measurements. The effect of interparticle interactions on the relaxation time is satisfactorily described by a superparamagnetic model where the dipolar energy is determined by a statistical calculation for a disordered arrangement of particles with volume distribution and easy axes in random orientations. The results indicate that the single particle anisotropy energy is mainly determined by surface anisotropy and that the energy barrier increases with the interaction strength. © **1998 John Wiley & Sons, Ltd.**

Appl. Organometal. Chem. **12**, 381–386 (1998)

Keywords: nanoparticles; magnetic susceptibility; magnetic anisotropy

Received 5 January 1998; accepted 11 February 1998

1 INTRODUCTION

Magnetic nanoparticles have raised much interest in recent years,[1–3] due to the modification of their properties with respect to the bulk materials, induced by size confinement (e.g. quantum tunneling of the magnetization) and surface and interface effects (e.g. improved soft and hard properties by exchange coupling through grain boundaries).

These differences have hardly been determined theoretically because of the difficulty of taking into account the complexity of real systems, where factors such as particle size and shape distribution, detailed geometrical arrangement, type and strength of interparticle interactions determine the actual magnetic behavior.[4,5] On the experimental side, the complication is related to the difficulty of making materials with a narrow size distribution, controlled dispersion of particles and limited aggregation.

In this paper we address these problems by analyzing the dynamical properties of various samples composed of γ-Fe_2O_3 particles embedded in a polymer, produced by a well-established technique[6] which allows us to control the parameters of the particle assembly. Our findings are obtained from the analysis of the dependence of dynamical magnetic susceptibility on temperature and frequency, and from Mössbauer spectra at various temperatures. Both of these techniques constitute a probe for the relaxation process of the magnetic moment of the particles, covering a large range of measuring time (10^{-8} s for Mössbauer; from 10^{-4} to 50 s for a.c. susceptibility). The results will provide evidence of the important role played by particle surface and interparticle interactions in determining the dynamical behavior.[5,7]

2 THEORY

The simplest situation to be considered is a single isolated particle (or an assembly of identical, non-interacting magnetic particles) with uniaxial anisotropy. In this case, according to the modified Néel–Brown formula, the relaxation time is given by Eqn [1],[8] where E_B is the total anisotropy energy barrier, k the Boltzmann constant and τ_0 is given by Eqn [2]. Here, V is the volume of the particle, $M_{nr}(0)$ is the non-relaxing magnetization at zero temperature, $_0$ is the gyromagnetic ratio for electrons, and η_r is related to the damping constant η through $_r = \eta\gamma_0 M_{nr}(0)$.

* Correspondence to: F. Lucari, Dipartimento di Fisica, Università Via Vetoio 10, I-67010 Coppito (L'Aquila), Italy.

 CCC 0268–2605/98/050381–06 $17.50

$$\tau = \tau_0 \exp(E_B/kT) \quad [1]$$

$$\tau_0 = \frac{\sqrt{\pi}}{4}\frac{VM_{nr}(0)}{E_B\gamma_0} \times \times \left[\frac{1}{\eta_r} + \eta_r\left(\frac{M_{nr}(T)}{M_{nr}(0)}\right)^2\right]\left(\frac{kT}{E_B}\right)^{1/2}\left(1+\frac{kT}{E_B}\right) \quad [2]$$

Often, the variation of τ_0 with temperature can be neglected with respect to the variation of the exponential. However, this dependence has to be considered when calculating the exact values of the parameters entering the τ expression.

The measurement of the a.c. susceptibility represents a very useful tool for investigating dynamical properties of magnetic nanoparticles, as it has the advantage of covering a large time window with the same technique. The real part of the complex susceptibility may be written as Eqn [3], extending Debye's theory of electric dispersion in dipolar fluids to the analogous case of non-interacting magnetic particles:[9]

$$\chi(\omega, T) = \frac{\chi_0 + \omega^2\tau^2\chi_1}{1+\omega^2\tau^2} \quad [3]$$

where

$$\chi_0 = \frac{VM_{nr}^2(T)}{3k(T-\theta_{sp})} \text{ and } \chi_1 = \frac{VM_{nr}^2(T)}{3E_B}$$

Here, χ_0 is the high-temperature superparamagnetic susceptibility, χ_1 the low-temperature blocked state susceptibility, and θ_{sp} the superparamagnetic temperature.

After substitution of Eqn [1] and considering that $_0$ is, for ferromagnetic or ferrimagnetic materials, of the order of $10^{-11} - 10^{-9}$ s, the susceptibility varies abruptly with temperature from the blocked to the superparamagnetic state. The transition temperature (blocking temperature, T_b) between the two regimes corresponds to the temperature at which $2\pi \simeq 1/\nu$, where $\nu = \omega/2\pi$, i.e.

$$T_b \approx \frac{E_B}{k \mid \ln 2\pi\nu\tau_0 \mid} \quad [4]$$

and corresponds, to a good approximation, to the maximum of the susceptibility. If the energy barrier is mainly determined by volume anisotropy (as for magnetocrystalline and magnetostatic anisotropy), then

$$E_B = K_v V \quad [5]$$

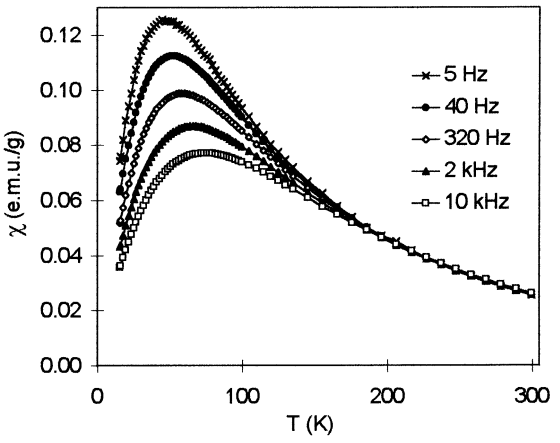

Figure 1 A.c. magnetic susceptibility (real part) as a function of temperature, measured at 1 Oe and various frequencies, for sample 4D IF.

where K_v is the anisotropy constant, and there is proportionality between blocking temperature and volume. However, as we will show later, surface contributions to anisotropy are essential to describe the actual situation.

When a distribution of particle volumes is present, the susceptibility is given by the volume-weighted sum of the individual contributions from each particle:

$$\chi(T,V) = \int_0^\infty \chi_V(T,V)Vf(V)\mathrm{d}V \Big/ \int_0^\infty Vf(V)\mathrm{d}V \quad [6]$$

where χ_v (T,V) is the susceptibility of the particles with volume V, and $f(V)$ is the particle distribution function. One expects, at a given frequency, a temperature dependence of the real magnetic susceptibility, with a peak at a certain value T_m. A typical plot is reported in Fig. 1. A characteristic volume in the distribution $V_c = R<V^2>/<V>$ exists, for which $T_b(V_c) = T_m$. The exact value of R depends on the shape (mainly the width) of the distribution. It is of the order of unity and has a negligible frequency dependence.[7,9]

The situation is more complicated for real fine particle systems where magnetic interparticle interactions are present. A regular arrangement of identical particles whose magnetic moments fluctuate with the same relaxation time does not describe the system, since the dynamics of the interactions is influenced by the random features of the system, including the magnetic moments, the distances, and the easy axis orientation of the

Table 1 Sample characteristics

Sample[a]	D (nm)	$<V^2>/<V>$ (nm^3)	n_1	d (nm)	$M_{nr}(0)$ (emu cm^{-3})	E_{Ba}/k (K)	$E_{B1}(0)/k$ (K)
36A IF (C/50)	4.6	75	1.7	23	240	530	—
18A CH (C/50)	4.8	105	3.0	24	250	585	155
3D IF (C/50)	6.8	300	1.1	34	280	850	—
32A IF (C/50)	6.9	333	1.2	34	290	835	—
33A IF (C/50)	7.1	372	1.3	35	300	1050	—
33A CH (C/50)	7.1	372	2.2	9	305	1050	470
33A IN (C/1)	7.1	372	12	11	370	1050	300
33A FL (C/50)	7.1	372	12	10	370	1050	400
4D IF (C/50)	7.9	550	1.1	38	300	935	—
4D I (C/25)	7.9	550	2.3	31	300	935	38
4D I (C/5)	7.9	550	8.3	20	300	935	130
4D IN (C/1)	7.9	550	12	13	300	935	275
35A IF (C/50)	8.7	572	1.3	43	300	930	—
26A IF (C/50)	10.1	950	2.0	50	350	1550	—

Key to symbols. D, average particle diameter; V, particle volume; n_1, number of first neighbors; d, interparticle distance; M_{nr}, non-relaxing magnetization; E_{Ba}, energy barrier for the particle alone; $E_{B1}(0)$, contribution per neighbor to the barrier due to interactions. For details, see the text.

[a] I, isolated; F, far; N, near; CH, chain; FL, floc. The number in parentheses refers to the nominal polymer-to-oxide mass ratio.

various particles. Actually, the interaction field also fluctuates, because of the distribution of relaxation times, and the anisotropic part of the interaction energy, which affects the effective energy barrier for magnetization reversal, changes in time. These peculiarities are considered in the model of Dormann *et al.*,[10] where the interaction energy is estimated by a statistical calculation. The total energy barrier for the magnetization reversal, with uniaxial anisotropy, is given by $E_B = E_{Ba} + E_{B,int}$, where the two terms are the energy for the isolated particle and the interaction energy, respectively.

In a first approximation, limited to interactions between first neighbors and to low temperatures, the exponential in Eqn [1] needs the substitution:

$$\exp(E_B/kT) \approx \exp(-n_1) \exp[(E_{Ba} + n_1 E_{B1})/kT] \quad [7]$$

where n_1 is the number of first-neighbor particles and E_{B1} is the contribution per neighbor to the energy barrier due to the interactions. For dipole interactions, at zero temperature, $E_{B1}(0) = M_{nr}^2(0)Va_1$, where $a_1 = V/d^3$ is the filling factor, d being the center-to-center interparticle distance.

The result is that an Arrhenius-like law for the relaxation time is still maintained but with a decrease in the pre-exponential factor from τ_0 to $_0 \exp(-n_1)$, which depends on the number of first neighbors, and an increase of the energy barrier E_B.

3 SAMPLE PREPARATION

The samples were prepared using the same chemical method,[6] which allows us to control the size of the particles and their state of dispersion in a polymer separately. Magnetite particles were prepared by making alkaline an aqueous mixture of $FeCl_2$ and $FeCl_3$ in a 1:2 molar ratio. The conditions in the precipitation medium control the size of the particles. Conversion into γ-Fe_2O_3 was obtained after repeated treatments in acidic medium. On dispersal in water, the γ-Fe_2O_3 particles yielded a sol. Large particles and agglomerates were removed after centrifugation. The pH of the sol was adjusted to 2–2.5, yielding a stable sol with minimum aggregation. Different states of aggregation up to flocculation were obtained by raising the pH step by step. The dispersions were solidified by adding a solution of polyvinyle alcohol and drying in air. The iron oxide/polymer mass ratio determines the volume fraction of the particles in the composite.

Transmission electron microscopy (TEM) observations were used to determine the particle size distribution and to characterize the state of aggregation. The particles are roughly spheroidal or ellipsoidal. Representative samples consist of quasi-isolated particles with $d \approx 1.5D$ (samples IN) and $\approx 5D$ (samples IF), where D is the average diameter associated with the mean volume $<V>$, chains (CH samples) and large agglomerates where d is slightly larger than D because of adsorbed

water (Floc samples). The sample geometrical characteristics and the values of $M_{nr}(0)$ determined from magnetization measurements are listed in Table 1.

4 EXPERIMENTAL RESULTS

4.1 Non-interacting particle samples (IF)

A.c. susceptibility experiments were performed as a function of temperature (15–300 K) at different frequencies (5–10000 Hz) and fields (0.1–25 Oe) with a commercial 7130 LakeShore apparatus. Very low-frequency susceptibility measurements (0.02 Hz) were performed using the Lissajous pattern technique. For each χ vs T curve, the temperature of the maximum, T_m, was determined through a polynomial fitting of the data around the maximum. Mössbauer spectra were recorded with a conventional spectrometer and analyzed using a modeling procedure.

Typical a.c. real susceptibility curves at different measuring frequencies are shown in Fig. 1 for the sample 4D IF. The agreement between the frequency dependence of the blocking temperature and the Néel–Brown model (Eqns [1], [2]) is very good. The fits provide values of the anisotropy energy $E_B = E_{Ba}$ and the damping factor η_r.[5] The values of E_{Ba} for the various samples are given in Table 1, whereas the values of η_r are close to 0.1 for all the samples.

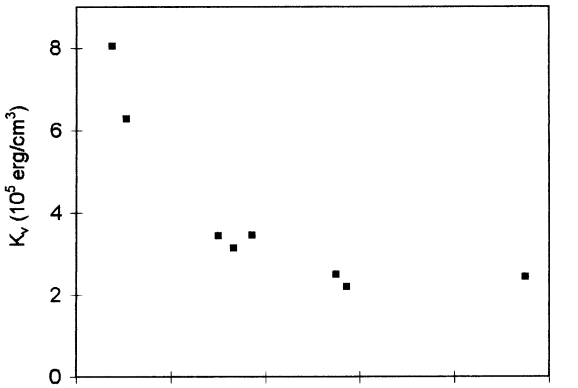

Figure 2 Volume anisotropy constant, calculated from Eqn [5], as a function of the volume of weakly interacting particles.

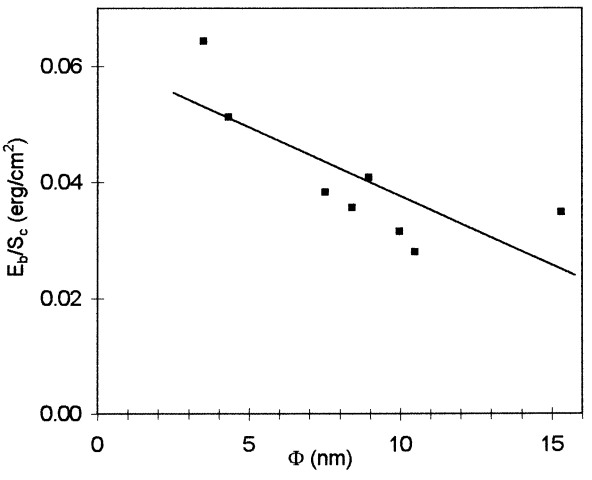

Figure 3 Ratio between the energy barrier E_B and the characteristic surface S_c (see the text) for some weakly interacting particle samples.

It is interesting to determine the kind of anisotropy governing E_B. The first assumption is to consider the volume anisotropy originated from magnetocrystalline and magnetostatic energy. The magnetocrystalline anisotropy (of cubic type) for γ-Fe_2O_3 is very weak, with a constant much smaller than 5×10^4 erg cm^{-3}. Therefore, the volume anisotropy can be taken as the magnetostatic anisotropy, with constant $K_{ma} = M_{nr}^2(T) \times (N_x - N_z)/2$, where N_x and N_z are the demagnetizing factors. An ellipticity of 0.7, as suggested by TEM observations, leads to $|K_{ma}| \simeq 10^5$ erg cm^{-3} for sample 33A IF, with small variations between the samples due to the differences in M_{nr} (Table 1).

Figure 2 represents the volume anisotropy constant derived from E_B and V_c for each sample, according to Eqn. [5]. Obviously, volume anisotropy is not consistent with the results. This suggests that the surface anisotropy plays an important role, adding to the magnetostatic anisotropy. As the two anisotropies have uniaxial symmetry with the same axis, we can write Eqn [8], where K_s is the surface

$$E_B = K_{ma} V_c + K_S Sc \qquad [8]$$

anisotropy constant, and S_c is the surface of a spherical particle with volume $V_c = R\ <V^2>/<V>$ (characteristic diameter ϕ_c). R was recalculated. In Fig. 3, E_B/S_c is plotted as a function of the effective diameter $\phi = \phi_c(M_{nr}/M_{nr,ref})^2$, accounting for the small differences in K_{ma} due to the differences in M_{nr} with respect to the reference sample 33A IF. We deduce $K_s = 0.06$ erg cm^{-2}, in very good

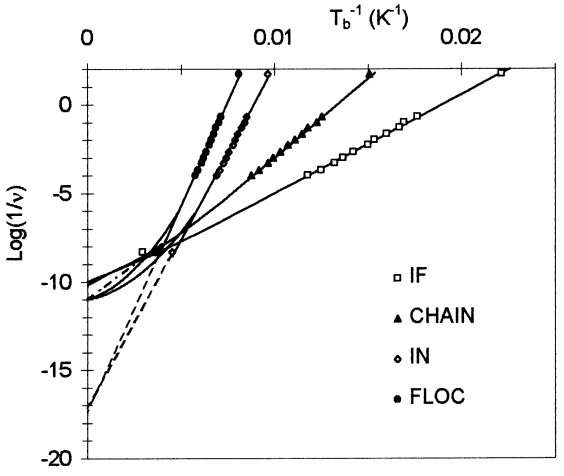

Figure 4 Dependence of the blocking temperature T_b on the measuring time $1/\nu$ for sample series 33A. The solid lines represent the results of the fitting; the broken lines are the extrapolation of the linear region (see the text).

agreement with the value deduced from the size dependence of the blocking temperature as measured by Mössbauer spectroscopy,[6] and $K_{ma} = -1.1 \times 10^5$ erg cm^{-3} for sample 33A IF, in very good agreement with the estimate, which clearly supports our analysis.[7]

4.2 Interacting particle samples

Figure 4 shows the dependence of T_b on the measuring time for the 33A series. The differences with respect to the IF sample are attributed to the presence of interparticle interactions. The data are fitted[5] very well using the Néel–Brown model for the τ expression (Eqns [1] and [2]) and our model[3,10] for the interaction effect. The intercept with the ordinate is related to the number of first neighbors (12 for the IN and Floc samples, ~2 for the CH sample) and the slope is related to the anisotropy energy, $E_B = E_{Ba} + n_1 E_{B1}(0)$, which clearly increases with interactions. $E_{B1}(0)$ (see Table 1) increases with decreasing interparticle distance. However, it is much larger than the value calculated for dipolar interactions. For example, for sample IN we find $E_{B1}(0) = 300$ K against 50 K for dipolar interactions. It is worth noting that, for isolated particles, $M_{nr}(0)$ decreases with decreasing the particle size, the effect being roughly proportional to the surface. $M_{nr}(0)$ also depends on the interactions. It is smaller than the bulk value (415 emu cm^{-3}) by 30% in the IF and CH samples, and only by 10% in the IN and Floc samples. The reduction is probably due to magnetic disorder at the particle surface,[11] which may be lower when interactions are present. This indicates that the surface energy varies with interactions and an extra surface-dependent term in the interaction energy is expected. The model is still valid if we make the substitution

$$E_{B1}(0) = a_1 M_{nr}^2(0) V + a_1 K_s' S \qquad [9]$$

The values of the surface additive term show that the surface anisotropy increases with the interaction strength,[5] due to modifications of the magnetic state at the particle surface.

In Fig. 5 we report the results for the 4D series, consisting of the same, quasi-isolated particles at different concentrations in the polymer matrix. A progressive increase of the energy barrier is observed as the concentration grows, and the same discussion holds as for the 33A series.[12] Again, the comparison between the experimental and the calculated interaction energy leads to the attribution of an important role to magnetic modifications of the surface under the effect of the interactions.

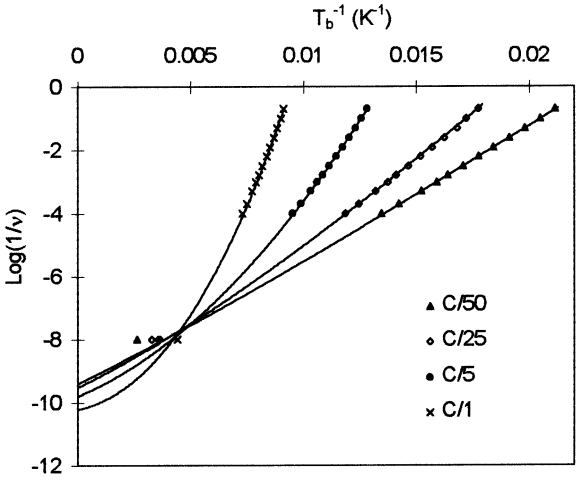

Figure 5 Dependence of the blocking temperature T_b on the measuring time $1/\nu$ for sample series 4D. The solid lines represent the results of the fitting (see the text).

5 CONCLUSIONS

Through the detailed analysis of the dynamical properties of a number of well-controlled dispersions of γ-Fe_2O_3 particles in a polymer, we have shown that the main contribution to the single

particle magnetic anisotropy is due to surface anisotropy and that interparticle dipolar interactions lead to an increase in the anisotropy energy barrier. Moreover, surface energy also affects interparticle interactions, changing with them and leading to an extra term which adds to the dipolar interaction one.

REFERENCES

1. J. L. Dormann and D. Fiorani (eds), *Magnetic Properties of Fine Particles*, North-Holland, Amsterdam, 1992.
2. G. C. Hadjipanayis and R. W. Siegel (eds), *Nanophase Materials*, NATO ASI Series E, Vol. 260, Kluwer Academic Publishers, Dordrecht, 1994.
3. J. L. Dormann, D. Fiorani and E. Tronc, *Adv. Chem. Phys.* **98,** 283 (1997).
4. R. W. Chantrell, In: *Magnetic Hysteresis in Novel Magnetic Materials*, Hadjipanayis, G. C. (ed), Kluwer Academic Publishers, Dordrecht, 1997, p. 21.
5. J. L. Dormann, F. D'Orazio, F. Lucari, E. Tronc, P. Prené, J. P. Jolivet, D. Fiorani, R. Cherkaoui and M. Noguès, *Phys. Rev. B* **53,** 14291 (1996).
6. E. Tronc and J. P. Jolivet, *Mater. Sci. Forum* **235–238,** 659 (1997).
7. J. L. Dormann, F. D'Orazio, F. Lucari, L. Spinu, E. Tronc, P. Prené, J. P. Jolivet and D. Fiorani, *Mater. Sci. Forum* **235–238,** 669 (1997).
8. W. T. Coffey, D. S. F. Crothers, Yu. P. Kalmykov, E. S. Massawe and J. T. Waldron, *J. Magn. Magn. Mater.* **127,** L254 (1993).
9. J. I. Gittleman, B. Abeles and S. Bozowski, *Phys. Rev. B* **9,** 3891 (1974) and references therein.
10. J. L. Dormann, L. Bessais and D. Fiorani, *J. Phys. C* **21,** 2015 (1988).
11. R. H. Kodama, A. E. Berkowitz, E. J. McNiff, Jr and S. Foner, *Phys. Rev. Lett.* **77,** 394 (1996).
12. J. L. Dormann, L. Spinu, E. Tronc, J. P. Jolivet, F. Lucari, F. D'Orazio and D. Fiorani, *J. Magn. Magn. Mater.*, in press.

